International Interdisciplinary Congress on Renewable Energies, Industrial Maintenance, Mechatronics and Informatics
Booklets

RENIECYT 1702902 CONACYT

RENIECYT - LATINDEX - Research Gate - DULCINEA - CLASE - Sudoc - HISPANA - SHERPA UNIVERSIA - Google Scholar DOI - REDIB - Mendeley - DIALNET - ROAD - ORCID

Title: Synthesis and characterization of Zinc Oxide thin films deposited by Spray Pyrolysis technique for possible applications in solar cells

Authors: VÁZQUEZ-VALERDI, Diana Elizabeth, LUNA-LÓPEZ, José Alberto, ABUNDIZ-CISNEROS, Noemí and JUAREZ-DÍAZ, Gabriel

Editorial label ECORFAN: 607-8695
BCIERMMI Control Number: 2022-01
BCIERMMI Classification (2022): 261022-0001

Pages: 14
RNA: 03-2010-032610115700-14

ECORFAN-México, S.C.
143 – 50 Itzopan Street
La Florida, Ecatepec Municipality
Mexico State, 55120 Zipcode
Phone: +52 1 55 6159 2296
Skype: ecorfan-mexico.s.c.
E-mail: contacto@ecorfan.org
Facebook: ECORFAN-México S. C.
Twitter: @EcorfanC

www.ecorfan.org

Holdings
Mexico, Colombia, Guatemala, Bolivia, Cameroon, Democratic Republic of Congo, Spain, El Salvador, Ecuador, Taiwan, Peru, Paraguay, Nicaragua

Introduction

Zinc oxide is a transparent n-type semiconductor with a direct band gap of ~3.37 eV and an exciton energy of 60 meV at room temperature [1, 2] due to its unique physical characteristics, it is considered a material with **excellent optical and electrical properties**, further it is non-toxic and inexpensive due to its abundance in the nature [3, 4].

Others positive properties include high electrochemical and thermal stability [4, 5]. For all these properties, the ZnO has generated special interest between the researchers for its use in optoelectronic devices.

The main crystalline structures that ZnO presents are the hexagonal wurtzite and zincblende [6, 7, 8]. ZnO films have been obtained by various techniques such as sputtering [9, 10], electron beam evaporation [11], spin coating, chemical vapor deposition, sol-gel [8] and ultrasonic spray pyrolysis (USP). [6, 12].

In the present study, the ZnO thin films have been deposited by SPU technique due to its low cost, simplicity (no high vacuum requirement, deposition shorts times), versatility and deposition uniformity [6].

The objective of this work is synthesized and characterized ZnO thin films deposited by Ultrasonic Spray Pyrolysis technique as possible candidate for electron transport layer (ETL),

integral part in solar cell, which offers the electron contact selectivity and mitigates recombination phenomena for enhanced device performance by its relatively high electron mobility, environmental stability, and transmissivity in the visible region [8, 13, 14].

There are many studies using ZnO in solar cells, such as ZnO nanowires, ZnO nanorods, ZnO nanoparticles and ZnO films, [14, 15, 16] that help improve device performance.

However in these studies, the complexity of the methods, the high temperature sintering process, the sophisticated, time consuming processing used for the obtained of the ETL are the disadvantage principal.

For all this reason, we considered that the ZnO thin films obtained by SPU technique

have a big potential to be used as ETL in solar cells.

Methodology

The ZnO was synthesized at a deposited temperature (Td) of 300, 350 and 400°C by the Ultrasonic Spray Pyrolysis technique.

- The thin films were deposited on glass and n-type silicon substrates, orientation (1 0 0), with a resistivity of 1-10 Ω cm.

The precursor solution was obtained using a molarity of 0.2 M of zinc acetate dihydrate [Zn $(CH_3COO)_2$ $2H_2O$] ≥98% dissolved in 50 ml methanol.

- The flow rate of solution was of 0.5 ml/min. The nozzle to substrate distance was 15 cm and diameter of nozzle was 2 cm. The deposition time was of 10 minutes for all samples.

The structural properties were investigated by X-ray Diffraction (XRD), a Diffractometer Bruker model D8 Discover equipped with ray X tube of Cu Kα radiation (λ=1.54059 Å), operated to 40 kV and 40 mA was used.

- The XRD patterns of ZnO thin films were recorded at grazing incidence measurements with an angle θ-2θ of 1°.

The optical properties were investigated by UV-Vis Spectroscopy, a Spectrophotometer Perkin Elmer 330, speed 120nm/min was used. Spectroscopic ellipsometry (SE), J.A. Woollam, M-2000DI.

- The ellipsometric parameter (amplitude Ψ and phase Δ) were acquired using an incidence angle of ~70 in a 193-1690nm spectral range.

The electrical properties were obtained by Hall Effect Measurement System, HMS-5000 at room temperature with a Magnetic Flux density of 0.5T.

Results

Graph 1 show the XRD patterns of ZnO thin films obtained at 300, 350 and 400°C. According to the peak positions matched in the (00-036-1451) PDF database the ZnO films have a hexagonal wurtzite structure with a preferential orientation (101). As the films were processed at different temperatures (300, 350, 400°C) the intensity of the XRD peaks were increased.

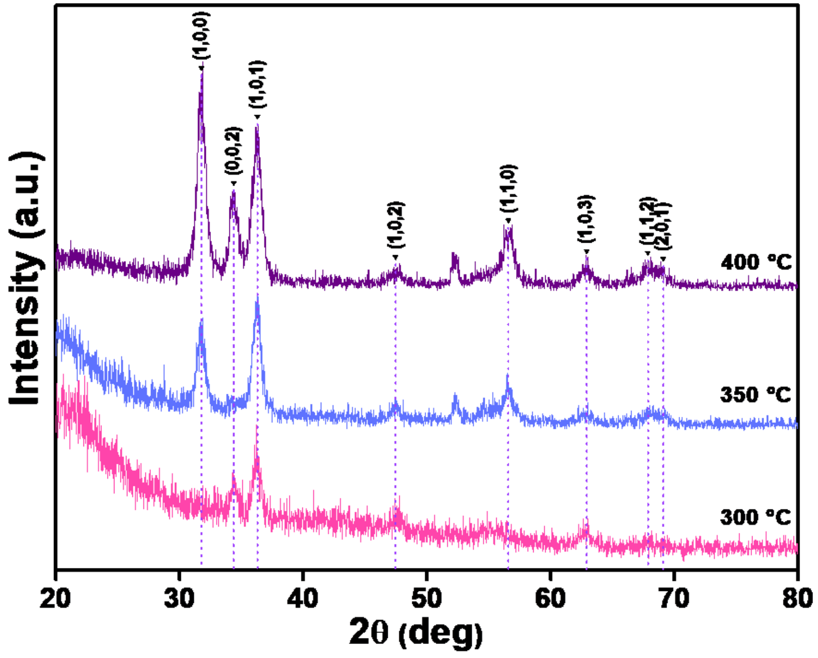

Graph 1 *XRD patterns of ZnO thin films obtained at 300, 350 and 400°C*

The observed XRD profile allow calculating the average crystallite size from peak (101). The X-ray diffraction peak broadening acquired in a diffractometer is due to the instrumental and the physical factors (as the crystallite size). The breadth that depends solely on the physical factors is extracted by subtracting the instrumental broadening factor from the experimental line profile according to [17]:

$$\beta = B\left(1 - \frac{b^2}{B^2}\right) \text{ (rad)} \quad (1)$$

2θ is the diffraction angle. B and b are the breadths of the peak from the XRD pattern at the same position of the experimental and reference sample respectively. The average diameter of the crystallites was calculated using Scherrer equation:

$$L = \frac{D\lambda}{\beta cos\theta} \quad (2)$$

where θ is the Bragg angle, λ is the X-ray wavelength (CuKa radiation) = 1.54056 Å, L is the crystal size, and D is the shape factor which is approximately the unity.

Graph 2 shows crystallite size by Scherrer equation of ZnO thin films obtained at 300, 350 and 400°C. The size of the obtained crystallites decreases as the temperature increases; however, the number of crystallites increases as indicated by the change in the intensity of the peaks.

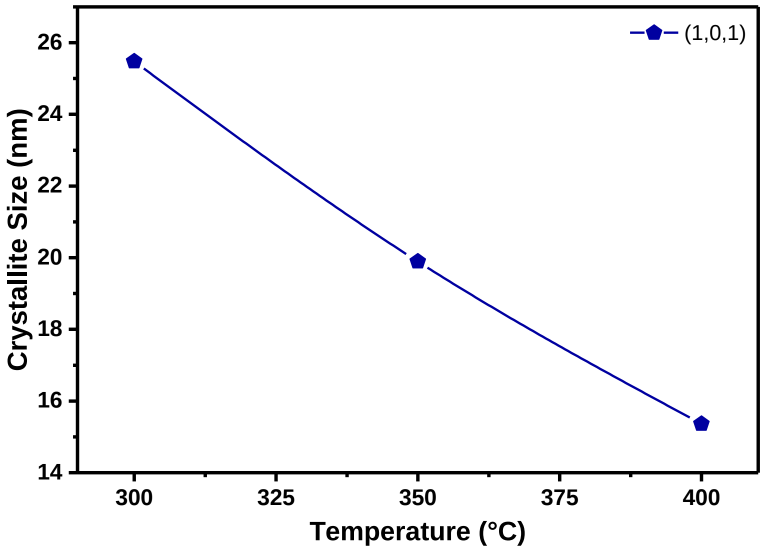

Graph 2 *Crystallite size by Scherrer equation of ZnO thin films obtained at 300, 350 and 400°C*

ZnO thin films were characterized by Spectroscopic Ellipsometry (SE), which is a frequently used optical characterization method for materials and nanoscale systems. It is based on measuring the change in the polarization state of a linearly polarized beam of light reflected from the sample surface. The ellipsometry spectra obtained from the Ψ and Δ parameters are fitted with an appropriate optical model for nanostructure thin film, and thus, rich information including surface roughness, film thickness, and optical constants of the nanomaterial are revealed [18].

Graph 3 show the complex refractive index (n and k) of ZnO thin films deposited at 300, 350 and 400°C. To obtain the optical properties the Gaussian oscillator model was used by the Complete EASE software.

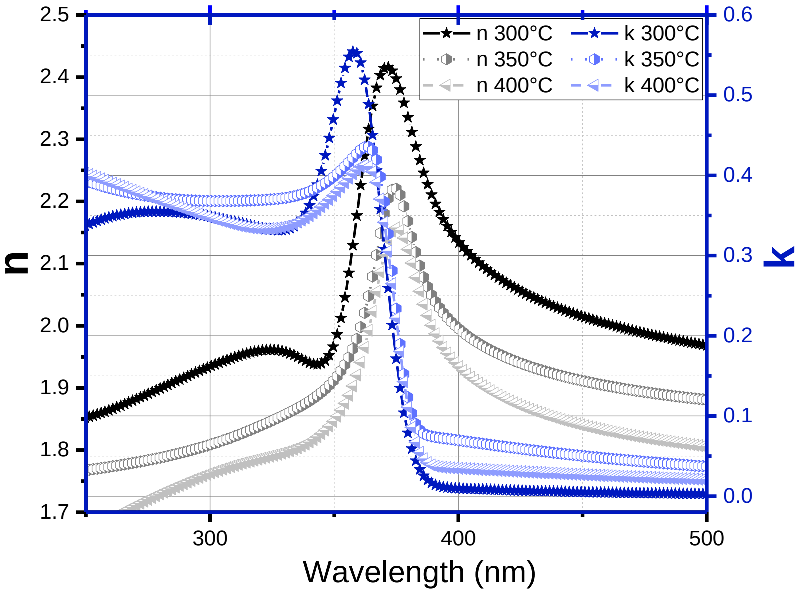

Graph 3 *Complex Refractive index (n and k) of ZnO thin films obtained at 300, 350 and 400°C.*

Table 1 show the thickness, surface roughness, complex refractive index (n and k) of the ZnO samples deposited at 300, 350 and 400°C.

Td (°C)	Thickness (nm)	Roughness (nm)	n@370nm	k@360nm
300	205±2.05	29.28±1.12	2.4	0.54
350	128.81±0.80	28.33±0.230	2.2	0.43
400	121.23±1.59	12.01±1.98	2.11	0.41

Table 1 *Values of thickness, surface roughness, complex refractive index (n and k) of ZnO samples deposited at 300, 350 and 400 °C.*

The thicknesses and roughness of the films decrease as the temperature increases even though the deposition time was constant. All the films showed a refractive index (n) greater than 2 in λ equal to 370nm (see table 1 and graph 3). Both, n and k increase towards lower energies, however for wavelengths greater than 370 nm these parameters tend to decrease, observing this behavior for all films. These changes in the optical properties can be associated with variations in the crystal structure and superficial morphology of the ZnO films [19, 20].

Graph 4 show the Transmittance spectra of the ZnO thin films. The optical characterization of the material showed a high transmittance in the visible region (85-99%). The figure inset in the graph 4 shows the absorption edge (404nm) of the samples.

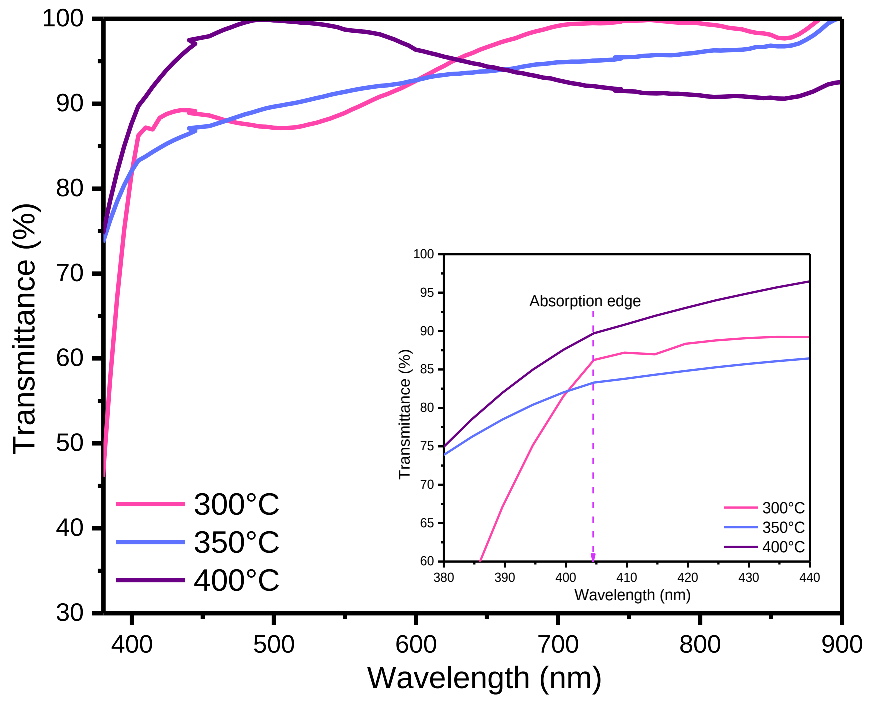

Graph 4 *Transmittance spectrum of ZnO thin films obtained at 300, 350 and 400°C. Inset absorption edge.*

Graph 5 shows the band gap calculated by means of transmittance spectrum and the relationship known as Tauc plot [21], considered a direct transition. The band gap (Eg) obtained was of 3.15 eV for the sample deposited at 300°C, which has a shift towards lower energies. For the case of the samples deposited at 350°C the Eg was of 3.06 eV and for the sample deposited at 400°C was of 3.29 eV.

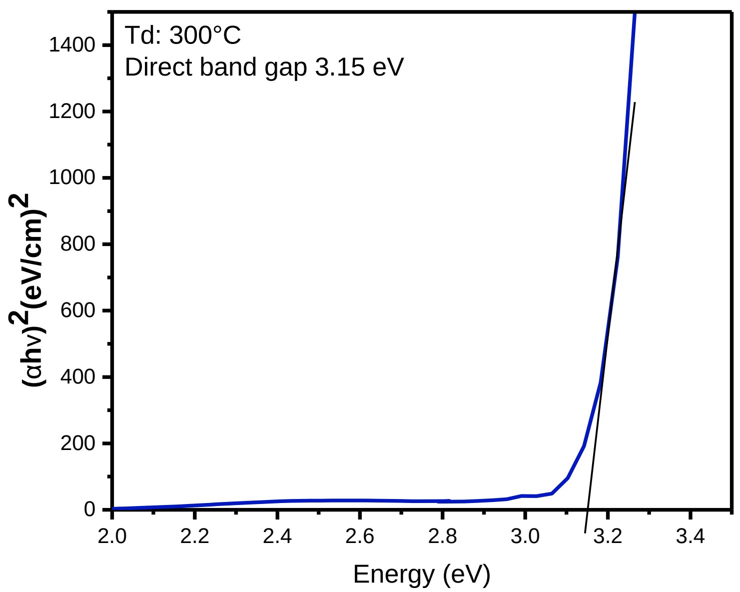

Graph 5 *$(\alpha h\nu)^2$ versus energy (hv). Example to obtain the Eg approximated value by using the relationship known as Tauc plot of ZnO thin film deposited at 300 °C*

The electrical properties of the ZnO thin films were obtained by Hall Effect measurement system, which revealed a low resistivity of 1-4 Ω cm for all samples and a relativity high electron mobility of charge carriers of 304 cm^2/Vs in the films.

Analysis

From XRD analysis: ZnO-hexagonal wurtzite phase with a preferential orientation (101) and that the mean crystallites size decreases of 25nm to 15mn as the deposition temperature increases of 300 to 400°C

Film deposited at 400°C has two possible orientations (interesting in its electrical properties).

Thicknesses and surface roughness of the films decrease of 200 to 120 nm and of 29 to 12 nm, respectively, as the temperature increases, which are related with the crystallite and grain size.

These results confirm that the thickness of the films can be controlled through the deposit temperatura (lower thickness, there is a mitigated recombination phenomena for enhanced device performance [22]).

The samples showed a high transmittance in the visible region (85-99%), which is optimal for the application as ETL (band gap, it could be modulated with the change of the deposition temperature).

The electrical measurements, which revealed a low resistivity of 1-4 Ω cm and a relativity high electron mobility of charge carriers of 304 cm2/Vs in all the films. This is an expected results due to the material nature.

Due to all these properties, ZnO thin films are considered a material with a big potential for to be used as ETL in solar cells.

Conclusions

- Highly transparent ZnO thin films were successfully prepared by the Ultrasonic Spray Pyrolysis technique on glass and n-type silicon substrates at 300, 350 and 400 °C, using solution of zinc acetate dihydrate.
- The X-ray diffraction analysis showed that films are polycrystalline nature with hexagonal wurtzite phase (preferential orientation (101)). The crystallites size is estimated of 25 to 15 nm.
- Optical measurements show that the films possess high transmittance over 85 % in the visible region and sharp absorption edge near 400 nm. The film has a direct band gap with an optical value of 3.06 to 3.29 eV which is close to the previously reported value (3.37 eV).
- Electrical results revealed a low resistivity of 1-4 Ω cm and a relativity high electron mobility of charge carriers of 304 cm2/Vs in all the films.
- The properties of the ZnO thin film can be controlled through the deposit temperature, which allowed found the best characteristics for obtained the electron transport layer as integral part of the solar cell.

References

[1] Kamarulzaman, N., Kasim, M., & Rusdi, R. (2015). Band gap narrowing and widening of ZnO nanostructures and doped. Materials. *Nanoscale Research Letters*, *10*(1) https://doi.org/10.1186/s11671-015-1034-9

[2] Muchuweni, E., Sathiaraj, T., & Nyakotyo, H. (2017). Synthesis and characterization of zinc oxide thin films for optoelectronic applications. *Heliyon*, *3*(4), e00285. https://doi.org/10.1016/j.heliyon.2017.e00285

[3] Muchuweni, E., Sathiaraj, T. & Nyakotyo, H. (2016). Physical properties of gallium and aluminium co-doped zinc oxide thin films deposited at different radio frequency magnetron sputtering power. *Ceramics International*, *42*(15), 17706–17710. https://doi.org/10.1016/j.ceramint.2016.08.091

[4] Malekkiani, M., Heshmati Jannat Magham, A., Ravari, F., & Dadmehr, M. (2022). Facile fabrication of ternary MWCNTs/ZnO/Chitosan nanocomposite for enhanced photocatalytic degradation of methylene blue and antibacterial activity. *Scientific Reports*, *12*(1). https://doi.org/10.1038/s41598-022-09571-5

[5] Li, F., Li, P., & Zhang, H. (2021). Preparation and Research of a high-performance ZnO/SnO2 humidity Sensor. *Sensors*, *22*(1), 293. https://doi.org/10.3390/s22010293

[6] Muchuweni, E., Sathiaraj, T. & Nyakotyo, H. (2016). Effect of gallium doping on the structural, optical and electrical properties of zinc oxide thin films prepared by spray pyrolysis. *Ceramics International*, *42*(8), 10066–10070. https://doi.org/10.1016/j.ceramint.2016.03.110

[7] Fan, W., Abiyasa, A., Tan, S., Yu, S., Sun, X., & Xia, J. et al. (2006). Electronic structures of wurtzite ZnO and ZnO/MgZnO quantum well. *Journal of Crystal Growth*, *287*(1), 28-33. *https://doi.org/10.1016/j.jcrysgro.2005.10.037*

[8] Ashrafi, A., & Jagadish, C. (2007). Review of zincblende ZnO: Stability of metastable ZnO phases. *Journal of Applied Physics*, *102*(7), 071101. https://doi.org/10.1063/1.2787957

[9] Nunes, P., Costa, D., Fortunato, E., & Martins, R. (2002). Performances presented by zinc oxide thin films deposited by R. F. magnetron sputtering. *Vacuum*, *64* (3-4), 293–297. https://doi.org/10.1016/s0042-207x(01)00323-2

[10] Saha, B., Das, N., & Chattopadhyay, K. (2014). Combined effect of oxygen deficient point defects and Ni doping in radio frequency magnetron sputtering deposited ZnO thin films. *Thin Solid Films*, *562*, 37-42. https://doi.org/10.1016/j.tsf.2014.03.038

[11] Choi, W., Kim, E., Seong, S., Kim, Y., Park, C., & Hahn, S. (2009). Optical and structural properties of ZnO/TiO2/ZnO multi-layers prepared via electron beam evaporation. *Vacuum*, *83*(5), 878–882. https://doi.org/10.1016/j.vacuum.2008.09.006
[12] Maciąg, A., Sagan, P., Kuźma, M., & Popovych, V. (2016). Zinc oxide films prepared by spray pyrolysis. *The European Physical Journal Conferences*, *133*:03004. *https://doi.org/10.1051/epjconf/201713303004*
[13] Caglar, M., Ilican, S., Caglar, Y., & Yakuphanoglu, F. (2009). Electrical conductivity and optical properties of ZnO nanostructured thin film. *Applied Surface Science*, *255*(8), 4491–4496. *https://doi.org/10.1016/j.apsusc.2008.11.055*
[14] Mahmud, M., Elumalai, N., Upama, M., Wang, D., Chan, K., & Wright, M. et al. (2017). Low temperature processed ZnO thin film as electron transport layer for efficient perovskite solar cells. *Solar Energy Materials and Solar Cells*, *159*, 251-264. https://doi.org/10.1016/j.solmat.2016.09.014
[15] Huang, J., Yin, Z. & Zheng, Q. (2011). Applications of ZnO in organic and hybrid solar cells. *Energy &Amp; Environmental Science*, *4*(10), 3861. *https://doi.org/10.1039/c1ee01873f*
[16] Luo, L., Lv, G., Li, B., Hu, X., Jin, L., Wang, J., & Tang, Y. (2010). Formation of aligned ZnO nanotube arrays by chemical etching and coupling with CdSe for photovoltaic application. *Thin Solid Films*, *518*(18), 5146-5152. https://doi.org/10.1016/j.tsf.2010.03.014
[17] Varin, R., Bystrzycki, J., & Calka, A. (1999). Effect of annealing on the microstructure, ordering and microhardness of ball milled cubic (L12) titanium trialuminide intermetallic powder. *Intermetallics*, *7*(7), 785-796. https://doi.org/10.1016/s0966-9795(98)00127-7
[18] Woollam, J.A., Johs, B., Herzinger, C., Hilfiker, J., Synowicki, R. & Bungay, C. (1999). Overview of variable angle spectroscopic ellipsometry (VASE), part I: Basic theory and typical applications. SPIE Proceedings CR72, 3–28.
[19] Alfaro Cruz, M., Ceballos-Sanchez, O., Luévano-Hipólito, E. & Torres-Martínez, L. (2018). ZnO thin films deposited by RF magnetron sputtering: Effects of the annealing and atmosphere conditions on the photocatalytic hydrogen production. *International Journal of Hydrogen Energy*, *43*(22), 10301-10310. https://doi.org/10.1016/j.ijhydene.2018.04.054
[20] Liu, Y., Tung, S., K. & Hsieh, J. (2006). Influence of annealing on optical properties and surface structure of ZnO thin films. *Journal of Crystal Growth*, *287*(1), 105-111. https://doi.org/10.1016/j.jcrysgro.2005.10.052
[21] Luna López, J., Vázquez Valerdi, D., Benítez Lara, A., García Salgado, G., Hernández-de la Luz, A., & Morales Sánchez, A. et al. (2017). Optical and compositional properties of SiOx films deposited by HFCVD: Effect of the hydrogen flow. *Journal of Electronic Materials*, *46*(4), 2309-2322. https://doi.org/10.1007/s11664-016-5271-1
[22] Yan, X., & Li, J. (2022). Effect of film thickness of ZnO as the electron transport layer on the performance of organic photodetectors. *Optical Materials*, *128*, 112438. https://doi.org/10.1016/j.optmat.2022.112438

ECORFAN®